AIAA Guidance, Navigation, and Control Conference and Exhibit
15 - 18 August 2005, San Francisco, California

AIAA 2005-6148

Optimal Trajectory Reconfiguration and Retargeting for a Reusable Launch Vehicle

Patrick J. Shaffer* and I. Michael Ross†
Naval PostGraduate School, Monterey, CA, 93943, USA
Michael W. Oppenheimer‡ and David B. Doman§
AFRL/VACA, 2210 Eighth Street, Bldg. 146, Rm. 305, WPAFB, OH 45433-7531

Autonomous reusable launch vehicles (RLV) are being pursued as low-cost alternatives to expendable launch vehicles and the Shuttle. The employment of autonomous, reusable launch vehicles requires additional guidance and control robustness to fulfill the role of an adaptive human pilot, in the event of failures or unanticipated conditions. The guidance and control of these vehicles mandate new guidance strategies that are able to identify and adapt to vehicle failures during the flight and still return to earth safely. This work utilizes an online trim algorithm that provides the outer loop with the feasible range of Mach number and angle of attack, for which the vehicle can be rotationally trimmed. The algorithm allows one to include 6-degree-of-freedom (DOF) trim effects and constraints in a reduced order dynamical model which is used in the solution of an optimal control problem. A direct pseudospectral method is used to solve a two-point-boundary-value problem which determines the optimal entry trajectory subject to appropriate constraints such as normal load, dynamic pressure limits, heat load limits, and state dependent constraints.

I. Introduction

The class of failures considered in this work are those control surface failures that affect a vehicle's aerodynamic characteristics and the ability to control the vehicle. Nominal reentry trajectories that were designed for the nominal vehicle are not necessarily optimal or feasible following a control surface failure. The challenge is to reconfigure the inner loop control system to use the healthy control effectors to compensate for the undesired effects of the failed vehicle and to retarget the new trajectory based upon aerodynamic force data, that includes off-nominal trim effects, to achieve an acceptable landing.

This work demonstrates the application of a direct pseudospectral method to determine the optimal entry trajectory for an RLV for nominal conditions as well as for off-nominal conditions caused by vehicle control surface failures. Vehicle aerodynamic data is used in a reduced-order dynamical model to generate the trajectories. State-dependent Mach and angle of attack constraints are included in the optimization problem. These constraints are computed by forming a trim deficiency map, which displays regions in the Mach-angle of attack space where the vehicle can be rotationally trimmed. The boundary of the trimmable region is used as a constraint in the optimization problem, requiring that any reshaped trajectories lie in the trimmable region, if physically possible.

II. Vehicle Model and Control Failures

The RLV used in this work is a lifting body with four sets of aerodynamic control surfaces: rudders, body flaps, and inboard/ outboard elevons. The control surface deflection vector, also known as the effector vector, is identified as

$$\boldsymbol{\delta} = \left[\begin{array}{cccccccc} Elevon_{R(in)} & Elevon_{R(out)} & Elevon_{L(in)} & Elevon_{L(out)} & Flap_R & Flap_L & Rudder_R & Rudder_L \end{array} \right] \quad (1)$$

*CDR, United States Navy.
†Associate Professor, Department of Mechanical and Astronautical Engineering, Naval Postgraduate School
‡Electronics Engineer, Control Theory and Optimization Branch, Member AIAA
§Senior Aerospace Engineer, Control Theory and Optimization Branch, Associate Fellow AIAA

Report Documentation Page

Form Approved
OMB No. 0704-0188

1. REPORT DATE	2. REPORT TYPE	3. DATES COVERED
AUG 2005		**00-00-2005 to 00-00-2005**

4. TITLE AND SUBTITLE	5a. CONTRACT NUMBER
Optimal Trajectory Reconfiguration and Retargeting for a Reusable Launch Vehicle	5b. GRANT NUMBER
	5c. PROGRAM ELEMENT NUMBER
6. AUTHOR(S)	5d. PROJECT NUMBER
	5e. TASK NUMBER
	5f. WORK UNIT NUMBER
7. PERFORMING ORGANIZATION NAME(S) AND ADDRESS(ES) **Air Force Research Laboratory,Air Vehicles Directorate,Wright Patterson AFB,OH,45433**	8. PERFORMING ORGANIZATION REPORT NUMBER
9. SPONSORING/MONITORING AGENCY NAME(S) AND ADDRESS(ES)	10. SPONSOR/MONITOR'S ACRONYM(S)
	11. SPONSOR/MONITOR'S REPORT NUMBER(S)

12. DISTRIBUTION/AVAILABILITY STATEMENT
Approved for public release; distribution unlimited

13. SUPPLEMENTARY NOTES
The original document contains color images.

14. ABSTRACT

15. SUBJECT TERMS

16. SECURITY CLASSIFICATION OF:			17. LIMITATION OF ABSTRACT	18. NUMBER OF PAGES	19a. NAME OF RESPONSIBLE PERSON
a. REPORT **unclassified**	b. ABSTRACT **unclassified**	c. THIS PAGE **unclassified**		**14**	

Standard Form 298 (Rev. 8-98)
Prescribed by ANSI Std Z39-18

The RLV control surfaces are position limited and have maximum and minimum deflections in degrees as shown by the vectors below:

$$\begin{aligned} \boldsymbol{\delta}_{min} &= \begin{bmatrix} -30 & -30 & -30 & -30 & -15 & -15 & -60 & -30 \end{bmatrix} \\ \boldsymbol{\delta}_{max} &= \begin{bmatrix} 30 & 30 & 30 & 30 & 26 & 26 & 30 & 60 \end{bmatrix} \end{aligned} \tag{2}$$

Many published works deal with the subject of reconfigurable control following a control surface failure of the vehicle at some point in its mission. The purpose of reconfigurable control is to maintain control of a vehicle (when physically possible) in the event of failure or damage by using the healthy control surfaces to compensate for the undesired effects of the failed surfaces. For many cases, reconfigurable inner loop control is insufficient to recover a vehicle that also relies on an autonomous guidance system that follows a prescribed trajectory.[1] Significant changes to the aerodynamics and a possible lack of control power may force one to determine a new trajectory based on knowledge of the type of failure. Failures may result in changes in the constraints on the state, cost, control and path arguments that correspond to the problem of computing a new optimal trajectory for a failed vehicle. A replanned trajectory must be computed that provides the ability to complete a mission to a terminal objective in order to save the vehicle and crew. Traditional methods store the trajectory data for a limited set of pre-planned engine-out or control surface failure scenarios and require significant data storage for implementation.

This work develops an online trim algorithm that provides the outer loop with the feasible range of Mach number and angle of attack, for which the vehicle can be rotationally trimmed. The algorithm allows one to include 6-degree-of-freedom (DOF) trim effects and constraints in a reduced order dynamical model which is used in the solution of an optimal control problem. A direct pseudospectral method is used to solve a two-point-boundary-value problem which determines the optimal entry trajectory subject to appropriate constraints such as normal load, dynamic pressure limits, heat load limits or trim deficiency. The approach assumes online identification of the failure. Following the failure identification and characterization, the new effector vectors containing the upper and lower control surface bounds are passed to a trim deficiency algorithm which determines the new feasible ranges of Mach number and angle of attack, as well as optimized effector vectors over a wide range of Mach numbers and angles of attack. The trim constraints are passed to the trajectory algorithm as Mach-angle of attack constraints that must not be violated when determining an optimal trajectory. The trim deficiency algorithm also queries the vehicle aerodynamic database to provide new vehicle coefficients of lift and drag in Mach-angle of attack space. Note that these new lift and drag coefficients include the trim lift and drag contributions of the healthy control effectors as well as the lift and drag contributions from the failed effectors. The outer loop dynamical model employs reduced order equations of motion that use table lookups, that are interpolated, to determine lift and drag coefficients derived from the vehicle state (based on angle of attack and Mach number).

III. Dynamical Model For Trajectory Optimization

The equations of motion are a simplified version of the traditional spherical earth equations of motion. There are six equations representing the kinematics and the 3-DOF dynamics of the problem as adapted from Wiesel.[2] The equations of motion are:

Kinematics:

$$\begin{aligned} \dot{x} &= V\cos\beta\cos\gamma \\ \dot{y} &= V\sin\beta\cos\gamma \\ \dot{z} &= V\sin\gamma \end{aligned} \tag{3}$$

Dynamics:

$$\begin{aligned} \dot{V} &= -\tfrac{D}{m} - g\sin\gamma \\ \dot{\gamma} &= \tfrac{L\cos\sigma}{mV} - \tfrac{g\cos\gamma}{V} \\ \dot{\beta} &= \tfrac{L\sin\sigma}{mV} \end{aligned} \tag{4}$$

where x (down range), y (cross-range), and z (altitude) are the vehicle's position, γ is the flight path angle, β is the azimuth angle, and σ is the bank angle. Also, V is the velocity magnitude and α is the vehicle angle of attack. L and D are the lift and drag forces, respectively, and are represented by

$$\begin{aligned} L &= \tfrac{1}{2} C_L A_{ref} \rho V^2 \\ D &= \tfrac{1}{2} C_D A_{ref} \rho V^2 \end{aligned} \tag{5}$$

where C_L and C_D are the lift and drag coefficients, respectively, ρ is the freestream mass density, and A_{ref} is a characteristic area for the body.

In this work, the reduced order model employed assumes that the coefficients of lift and drag are functions of the state variables only so that $C_L, C_D = f(M, \alpha)$. This simplified assumption is valid because the vehicle is assumed to be in coordinated flight (trimmed in yaw, no sideslip) and the model performs a table lookup of the lift and drag coefficients that were obtained from a full order model that uses the vehicle flight condition and an optimized trim effector displacement vector as arguments to interpolate aerodynamic data for the vehicle. The resulting coefficients of lift and drag from wing, body, and trim effects are summed and incorporated into the table. The effector displacement is an implicit argument used to determine the coefficients of lift and drag. The use of the optimized effector vector effectively decouples the outer loop from the inner loop. A state vector is chosen that fully represents the state of this reduced-order model at any instant. Using a flat earth coordinate system, the position and state of the vehicle can be represented by

$$\mathbf{x} = \begin{bmatrix} x & y & z & V & \gamma & \beta \end{bmatrix}^T \tag{6}$$

The control vector for this problem is the vector whose elements are the controllable parameters (i.e. forces) of this reduced order system. Note that reentry is accomplished dead-stick, i.e., there is no thrust control variable. For symmetric flight (i.e. $\beta = 0$) the coefficients of lift and drag are determined by the vehicle's angle of attack and Mach number. The vehicle's bank angle when combined with angle of attack determines the vehicle's crossrange motion. A suitable candidate for the control vector is therefore

$$\mathbf{u} = \begin{bmatrix} \alpha & \sigma \end{bmatrix}^T \tag{7}$$

This type of control is also called inertialess control,[3] meaning that it is assumed that there exist no lags or delays between commanded changes to the control variables and a change in their actual position.

A. 4-DOF Model

The inertialess controller can be adapted to more accurately model the physical system by recognizing that α and σ have bandwidth and rate limitations. The inertialess assumption is relaxed by imposing realistic rate constraints on the actuators. This is accomplished by incorporating the elements of the control vector in Equation 7 into the state vector in Equation 6. The new state vector becomes the following 8-element vector:

$$\mathbf{x} = \begin{bmatrix} x & y & z & V & \gamma & \beta & \alpha & \sigma \end{bmatrix}^T \tag{8}$$

The new control vector components are now the rates of the previous control vector's components in Equation 7, so that,

$$\mathbf{u} = \begin{bmatrix} \dot{\alpha} & \dot{\sigma} \end{bmatrix}^T \tag{9}$$

This alternative formulation provides a more realistic model by preventing unlimited control surface deflection rates. Note that while the physical controls remain α and σ, the algorithm uses the rates of these variables in its optimization. The physical controls α and σ are perhaps better described as virtual controls and are primarily manipulated through the deployment of aerodynamic control surfaces. Thus actuator bandwidths, rate limits, and vehicle inertias all contribute to lags between the commands to the virtual controls and their responses.

B. RLV Aerodynamic Model

This work considers the atmospheric entry of the reusable launch vehicle following a mission in low-earth orbit. The computed trajectory is an unpowered descent to a known landing field. The trajectory exposes the vehicle to a wide range of Mach numbers and angles of attack. To accurately model the vehicle's aerodynamic performance, the trajectory optimization algorithm queries the aerodynamic data to determine the full order aerodynamic characteristics including wing-body and trim effects from an input vector consisting of Mach number, angle of attack, and control effector positions. Assuming that the vehicle is not maneuvering (small body angular rates), the position of the control effectors must be such that the vehicle is trimmed. It is worth pointing out that there may be more than one set of deflections that trim the vehicle at given Mach number and angle of attack. Thus, a piecewise linear programming (PLP)[4] algorithm is used to determine the optimal positions of the vehicle's control surfaces (i.e., control induced moments balance the moments generated by the wing-body with minimum control deflection in a 1-norm sense). Two-dimensional tables of total lift and drag coefficients in Mach-α space are then generated by the algorithm that include the contributions of the control effector deflections. Note that control failures cause these effector deflections to change and thus the trim lift and drag contributions of the effectors change under failure conditions. Additionally, the failures can also limit the feasible region of Mach-α space which must be translated into virtual control limits in the trajectory generation problem.

The control allocation algorithm is used to trim the vehicle. It is assumed that the vehicle is in symmetric flight (sideslip angle is zero) and the resulting lateral wing-body force and moment coefficients are zero. By assuming a zero magnitude body-axis angular velocity, the wing-body pitching moment of the vehicle becomes a function of Mach number and angle of attack. This allows for the following necessary condition to rotationally trim the vehicle: the moments resulting from all control surface deflections (failed and healthy) must be equal and opposite to the moments produced by the wing-body. Thus,

$$\begin{pmatrix} C_{rm_\delta}(M,\alpha,\boldsymbol{\delta}) \\ C_{m_\delta}(M,\alpha,\boldsymbol{\delta}) \\ C_{ym_\delta}(M,\alpha,\boldsymbol{\delta}) \end{pmatrix} = \begin{pmatrix} 0 \\ -C_{m_o}(M,\alpha) \\ 0 \end{pmatrix} \tag{10}$$

where $C_{rm_\delta}(M,\alpha,\boldsymbol{\delta})$, $C_{m_\delta}(M,\alpha,\boldsymbol{\delta})$, and $C_{ym_\delta}(M,\alpha,\boldsymbol{\delta})$ are the rolling, pitching, and yawing moment coefficients produced by the control effectors and $C_{m_o}(M,\alpha)$ is the wing-body pitching moment.

The first task of the control allocator is to determine the optimum effector displacement that results in minimum control deficiency. The full set of control surface deflections for the vehicle can be represented by the eight-element effector displacement vector in Equation 1. This vector is nominally subject to the limits of Equation 2 or by a modified set of position limits that reflect the current health of the effector suite. The control allocation problem uses an iterative algorithm that queries the full 6-DOF aerodynamic database. The piecewise linear constrained control allocation problem is

$$\min_{\boldsymbol{\delta}} J_D = \min_{\boldsymbol{\delta}} \left\| \begin{bmatrix} 0 \\ -C_{m_{oj,i}}(M_j,\alpha_i) \\ 0 \end{bmatrix} - \begin{bmatrix} C_{rm_{\delta j,i}}(M_j,\alpha_i,\boldsymbol{\delta}_{j,i}) \\ C_{m_{\delta j,i}}(M_j,\alpha_i,\boldsymbol{\delta}_{j,i}) \\ C_{ym_{\delta j,i}}(M_j,\alpha_i,\boldsymbol{\delta}_{j,i}) \end{bmatrix} \right\|_1 \tag{11}$$

subject to

$$\boldsymbol{\delta}_{min} \leq \boldsymbol{\delta} \leq \boldsymbol{\delta}_{max} \tag{12}$$

at each Mach-α point in the aerodynamic database. Notice that the upper and lower bounds on $\boldsymbol{\delta}$ are dependent upon the operating mode of the vehicle. A vehicle operating under nominal conditions has the full range of deflections available while a vehicle operating with a control surface failure has a subset of the nominal displacement vector's range. A nonzero value for Equation 11 means that there is insufficient control power to rotationally trim the vehicle (it is trim deficient), and the vehicle will depart controlled flight. The trim deficient regions in Mach-α space can be mapped and identified as flight envelope boundaries that constrain the trajectory. If the control allocation algorithm is able to rotationally trim the vehicle, any excess control power can be used to maneuver the vehicle. The control allocator employs a second control allocation optimization algorithm to minimize the deviation from a minimum control deflection condition. This condition is represented by an eight-element preference vector set to zero and roughly corresponds to a minimum drag condition. The second optimization is

$$\min_{\boldsymbol{\delta}} J_S = \min_{\boldsymbol{\delta}} \|\mathbf{W}\left(\boldsymbol{\delta} - \boldsymbol{\delta}_p\right)\| \tag{13}$$

subject to

$$\boldsymbol{\delta}_{min} \leq \boldsymbol{\delta} \leq \boldsymbol{\delta}_{max} \tag{14}$$

and

$$\begin{pmatrix} C_{rm_\delta}(M,\alpha,\boldsymbol{\delta}) \\ C_{m_\delta}(M,\alpha,\boldsymbol{\delta}) \\ C_{ym_\delta}(M,\alpha,\boldsymbol{\delta}) \end{pmatrix} = \begin{pmatrix} 0 \\ -C_{m_o}(M,\alpha) \\ 0 \end{pmatrix} \tag{15}$$

In Equation 13, $\mathbf{W}$ is a weighting matrix used to weight the importance of driving an effector to its preferred location. In the case where the vehicle is operating with excess control power, the effector displacement vector is the output of the second optimization routine, otherwise $\boldsymbol{\delta}$ minimizes the trim deficiency. The effector displacement vector that is the solution of the control allocator is represented as $\boldsymbol{\delta}^*$ to delineate it from the possibly multiple combinations of control surface deflections that are available to achieve the same desired control but are not optimized for minimum control deflection.

Given $\boldsymbol{\delta}^*(\alpha, M)$ from the control allocation algorithm, the aerodynamic database is queried over the Mach-α grid to generate the wing-body and trim lift and drag coefficients. These coefficients, when summed together, represent the total lift and drag coefficients. The use of the control allocator solution effectively decouples the trajectory generation algorithm from the inner loop and allows the lift and drag coefficients to be functions of angle of attack and Mach number. Effector displacement remains an implicit argument and allows for the full 6-DOF model's behavior to be captured by a lower order model. The outer loop equation, namely, $C_L, C_D = f(M,\alpha)$ is evaluated using the lift and drag coefficients as the sum of the wing-body coefficients plus the effector-dependent trim coefficients using the control allocator solution. Thus,

$$\begin{aligned} C_L(M,\alpha) &= C_{L_o}(M,\alpha) + C_{L_{\delta^*}}(M,\alpha,\boldsymbol{\delta}^*) \\ C_D(M,\alpha) &= C_{D_o}(M,\alpha) + C_{D_{\delta^*}}(M,\alpha,\boldsymbol{\delta}^*) \end{aligned} \tag{16}$$

The relationships in Equation 16 hold for a vehicle in symmetric flight and can be stored in an aerodynamic lookup table for each Mach and angle of attack combination subject to the limits on the effector displacement vector dictated by the presence of nominal or failure conditions. Each failure condition requires a separate run of the control allocator.

IV. Trajectory Replanning Algorithm

The vehicle is assumed to operate in the nominal condition until a failure has been identified through some online fault detection or identification algorithm, at which point the lift and drag table corresponding to the failed vehicle configuration is generated. Once a failure has been identified, the control allocator generates a new set of control deflections for the failed vehicle and uses the aerodynamic database to determine the new trim lift and drag contributions. In the process of computing the control deflections for the failed vehicle, points in the Mach-α envelope for which the vehicle cannot be trimmed are identified. These trim deficiency regions must be avoided and are thus used as path constraints for the trajectory replanning. The aerodynamic data table is then changed to account for the current failed condition and a new trajectory is generated for the new aerodynamics and path constraints. Figures 1 and 2 show the trim deficiency maps for a nominal case and a case of both bodyflaps failed at 26°. In three-dimensions, Figure 2 becomes the plot shown in Figure 3. Notice, from Figure 1, that the maximum trim deficiency value is on the order of machine precision so that the entire range of combinations of angles of attack and Mach numbers is considered to be available in the nominal (unfailed) case. Hence, the entire Mach-α space is trimmable. When the bodyflaps are stuck at 26°, the envelope describing allowable Mach numbers-angles of attack is now severely reduced (see Figures 2 and 3). Points in the Mach-α envelope where the pitch deficiency is non-zero indicate an attitude which cannot be trimmed in pitch and is therefore uncontrollable. This establishes a restricted region that feasible trajectories must avoid. In other words, the trajectory must have a clear path in Mach-α space from the initial conditions to the final conditions. A clear path is defined as a path from one point defined by the flight condition (Mach-α) to another point (Mach-α) with no intervening regions of unacceptable trim deficiency. Should a path cross into or through a region of pitch deficiency, the trajectory becomes infeasible because the vehicle is no longer rotationally trimmable and is therefore uncontrollable.

Having obtained the control effector settings, that rotationally trim the vehicle, the changes to the trim lift and drag can be computed. Utilizing $\boldsymbol{\delta}^*(M,\alpha)$ from the control allocation problem, the aerodynamic

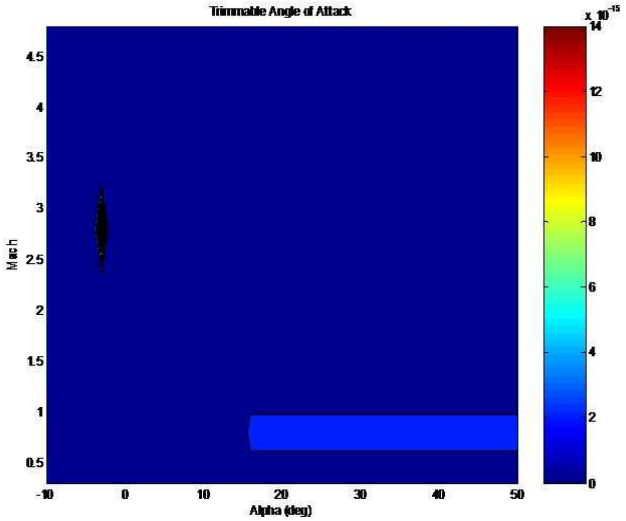

Figure 1. Pitch Deficiency For Nominal Vehicle.

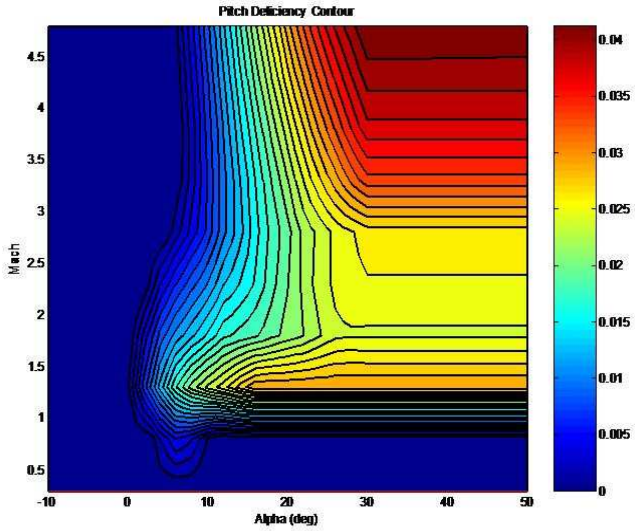

Figure 2. Pitch Deficiency For Failed Body Flaps at 26°**.**

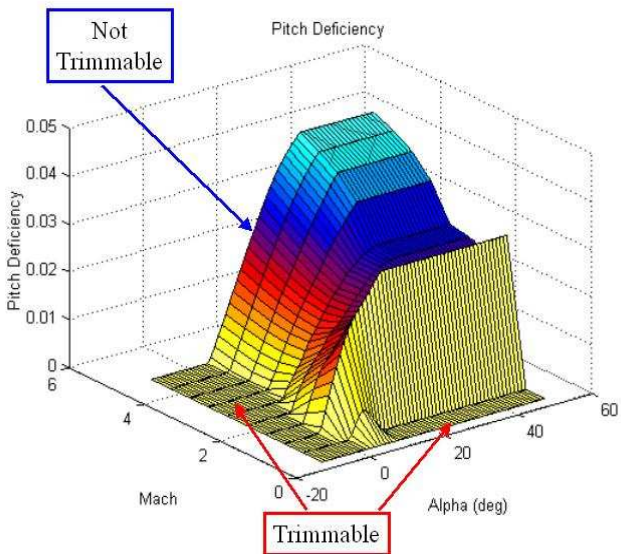

Figure 3. Three-Dimensional Pitch Deficiency For Failed Body Flaps at 26°.

database can be queried to determine the trim lift and drag perturbations. Figures 4 and 5 show the nominal and failed lift and drag maps over the entire Mach-α range of interest. In this case, the failure of the bodyflaps at 26° does not significantly affect the lift of the vehicle, however, large changes are seen in the drag. Given this information and the range of trimmable angle of attack, the portions of the lift and drag maps, which correspond to trimmable regions, can be identified. This information is then made available to a trajectory reshaping algorithm to ensure that a feasible trajectory, if one exists, is computed.

Note that the previous discussion does not consider any other limitations such as normal force, heating, or dynamic pressure on the trajectory. These constraints will further reduce the area available to a clear path for a feasible trajectory. In some cases, the additional constraints will completely eliminate a clear path. It is easier to visualize the optimal trajectory with constraints as a region through Mach-α space for which the vehicle must be rotationally trimmable. If a failure impinges on this corridor and prevents a clear path through to landing, then there are no feasible trajectories available.

The trim deficiency path constraint on the available range of angle of attacks for a given Mach number requires that the vehicle must be rotationally trimmable (assuming no side slip) for a given angle of attack. When the vehicle operates in a nominal configuration it is capable of trimming over a full range of angle of attack, however, when the vehicle experiences control degradation, its available range of angles of attack may be severely reduced.[5]

V. The Optimal Control Problem

Nearly any trajectory generation problem can be posed as an optimal control problem. Let the system, with dynamic constraints, be represented by

$$\dot{\mathbf{x}} = \mathbf{f}(\mathbf{x}, \mathbf{u}, \tau) \tag{17}$$

where $\mathbf{f}$ is a vector of functions that describe the dynamics of the system, $\mathbf{x}$ is a vector of states that fully describe the system at any time τ, and $\mathbf{u}$ is a vector of control variables. Assume the system is subjected to additional constraints to include the path constraint of the form

$$\mathbf{h}_l \leq \mathbf{h}(\mathbf{x}, \mathbf{u}, \tau) \leq \mathbf{h}_u \tag{18}$$

where $\mathbf{h}$ is a vector of functions describing the path constraints, $\mathbf{h}_l$ is a vector of lower path bounds, and $\mathbf{h}_u$ is a vector of upper path bounds. Additionally, the boundary conditions are specified as

$$\mathbf{e}_l \leq \mathbf{e}(\mathbf{x}(\tau_o), \mathbf{x}(\tau_f), \tau_o, \tau_f) \leq \mathbf{e}_u \tag{19}$$

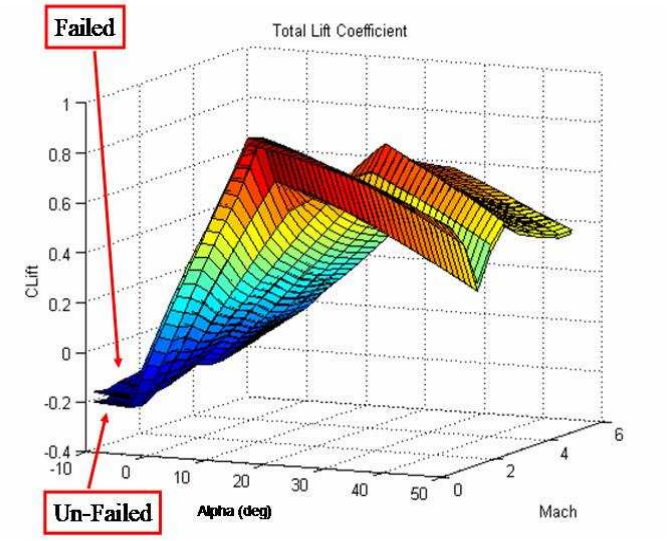

Figure 4. Nominal and Bodyflap Failure Lift Map.

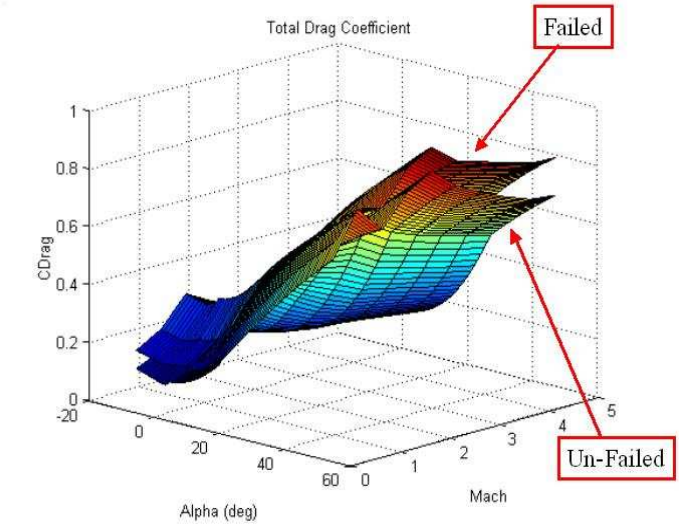

Figure 5. Nominal and Bodyflap Failure Drag Map.

where $\mathbf{e}(\mathbf{x}(\tau_o), \tau_o)$ is a vector of initial boundary conditions at τ_o, $\mathbf{e}(\mathbf{x}(\tau_f), \tau_f)$ is a vector of final boundary conditions at τ_f, $\mathbf{e}_l$ is a vector of lower bounds, and $\mathbf{e}_u$ is a vector of upper bounds. Similarly, the system also has bounds on the control and state variables represented by

$$\begin{aligned} \mathbf{x}_l \leq \mathbf{x}(\tau) \leq \mathbf{x}_u \\ \mathbf{u}_l(\mathbf{x}) \leq \mathbf{u}(\tau) \leq \mathbf{u}_u(\mathbf{x}) \end{aligned} \tag{20}$$

The bounds on the state and control vectors can be thought of as connecting the physical system being modelled to the mathematical model used to solve the optimal control problem. For example, if the control is acceleration, no physically realizable device produces infinite acceleration and we therefore may choose to limit the control to a sensible value. Similarly, if one element of the state vector is velocity, we must limit the velocity to values that are within the design limits of the physical system. Imposing constraints on the state and control vectors may not be necessary in all cases but the resulting optimal solution of unbounded states or controls needs to be given a hard reality check when realizing a physical implementation of the optimal solution.

An optimal control problem seeks to determine the solution of the preceding dynamical system with its bounds and constraints to minimize a given performance index. The general optimal control problem is fully posed in the following manner

$$\min_u J(\mathbf{x}(\tau), \mathbf{u}(\tau), \tau_o, \tau_f) = E(\mathbf{x}(\tau_o), \mathbf{x}(\tau_f), \tau_o, \tau_f) + \int_{\tau_o}^{\tau_f} F(\mathbf{x}(\tau), \mathbf{u}(\tau), \tau) d\tau \tag{21}$$

subject to

$$\begin{aligned} \dot{\mathbf{x}} = \mathbf{f}(\mathbf{x}, \mathbf{u}, \tau) \\ \mathbf{h}_l \leq \mathbf{h}(\mathbf{x}, \mathbf{u}, \tau) \leq \mathbf{h}_u \\ \mathbf{e}_l \leq \mathbf{e}(\mathbf{x}(\tau_o), \mathbf{x}(\tau_f), \tau_o, \tau_f) \leq \mathbf{e}_u \\ \mathbf{x}_l \leq \mathbf{x}(\tau) \leq \mathbf{x}_u \\ \mathbf{u}_l(\mathbf{x}) \leq \mathbf{u}(\tau) \leq \mathbf{u}_u(\mathbf{x}) \end{aligned} \tag{22}$$

where E is a scalar cost function evaluated at the boundaries and F is a scalar cost function evaluated over the entire interval. When J consists of only E, the cost function is in Mayer form. When J consists of only F, the cost function is in Lagrange form. When both E and F are present, the cost function is in Bolza form. The formulation of the system as represented in the state vector, the appropriate choice of the dynamical equations, and the selections of the constraints and bounds forms the basis of the fully posed optimal control problem.

A. Solution Methodology

Once the problem has been properly formulated there are two general methods available to solve the optimal control problem, direct and indirect.[6] Indirect methods tend to generate fast solution times and greater accuracy but are considerably more difficult to formulate and are very sensitive to the initial guess.[6] Formulation of the indirect method can be exceedingly difficult in situations where the dynamics functions are not pure functions but instead rely on numerical data such as the aerodynamic lookup tables used in this work.

Direct methods reduce the optimal control problem to a single large Nonlinear Programming (NLP) problem. The strengths of the direct methods are that the formulation is significantly easier and the methods are relatively insensitive to the initial guess. A particular drawback of direct methods is large execution times. When direct methods are used, there are tradeoffs between execution time and accuracy. An increase in the size of the NLP program does not necessarily yield a proportional increase in solution accuracy or solution time. This drawback inhibits real time optimal control using direct methods for certain problems such as are considered here; however, as computing power continues to increase, the potential for real time optimal control may soon be realized.

This work uses the DIDO numerical dynamic optimization software developed by I.M. Ross and F. Fahroo of the Naval Postgraduate School. DIDO employs a direct Legendre psuedospectral[7–12] technique that uses the NLP solver SNOPT. Since the formulation of a problem using a direct Legendre psuedospectral method does not determine the adjoint equations, another tool must be employed to link the solutions generated

by indirect methods and direct methods. The Covector Mapping Theorem (CMT)[6] provides this link. The implications of the CMT allow a determination of the optimality of a given solution by comparing the costates of the solution to the Karush-Kuhn-Tucker (KKT) multipliers. Every time a state or control becomes bounded, the corresponding costate should follow the KKT conditions as if they were the KKT multipliers. Additional evidence of optimality can be obtained by investigating the solution's Hamiltonian and the final value of the cost function. These necessary conditions may be easily obtained from the DIDO solution and provide insight into the optimality of the DIDO generated solution.

Because the DIDO solution is based upon the controls for a discretized set of points determined by the Legendre polynomials used in the solution, the DIDO solution may not possess the desired accuracy at the final endpoint. Since the accuracy of a DIDO solution is a function of the number of nodes evaluated in the solution space, all DIDO solutions should be evaluated for feasibility. This is usually accomplished by comparing the DIDO solution to a separate solution using the DIDO controls propagated by a Runge Kutta ODE solver such as MATLAB's ODE45. The error between the propagated states and the DIDO-derived states gives some measure of confidence of the accuracy of the DIDO solution. The required accuracy is determined by the application, for example while the downrange accuracy of a 20-node DIDO solution reentry trajectory is 0.0001% of the propagated downrange distance, it still may be inaccurate enough to prevent a feasible landing at the desired field. Feedback may be able to overcome this inaccuracy provided the solution update is achieved at a reasonable rate. Another guard against inaccuracies in a trajectory is to provide additional margins when defining the endpoint conditions.

While direct methods are relatively insensitive to the initial guess, a well-formulated problem can be completely ruined by improper scaling and balancing of the variables and constants used in the computation. The intent of scaling and balancing is to avoid the problems associated with variables whose range exceeds that of numerical precision. A properly scaled problem scales the variables to a range of 0 to 1. While it is not necessary to be exactly within this range, it is clear that variables of the same order of magnitude avoid problems associated with computing ill-conditioned matrices resulting from numerical imprecision. The optimization problems solved in this work have been scaled and balanced.

VI. Re-entry Optimal Control Problem

The reentry problem considers a vehicle entering the atmosphere from an initial position, presumably near low earth orbit and seeks to generate an optimal trajectory that brings it to a final state specified by an endpoint condition. The trajectory may not violate the path constraints which limit heating rate, normal force, and dynamic pressure. The optimal trajectory seeks to minimize a performance index which is generally a function of the state of the vehicle. Typical performance indices for reentry are maximizing downrange, maximizing cross range, minimizing control effort, or some weighted combination of these indices.

The trajectory is also subject to dynamic constraints which describe the dynamics of the system. As discussed in the previous section, this work uses a simple dynamic model that retains the benefits of a higher fidelity model by including the effects of trim lift and drag and using table lookups in a high-fidelity aerodynamic database.

For a typical trajectory that seeks to determine the maximum downrange value for an entering vehicle, the cost function is simply a Mayer cost:

$$J(\mathbf{x}(t), \mathbf{u}(t), t_0, t_f) = -x_f \tag{23}$$

The initial boundary conditions for a representative mission are

$$\mathbf{e}(\mathbf{x}(t_0), t_0) = \mathbf{x}_i = \begin{pmatrix} x_i \\ y_i \\ z_i \\ V_i \\ \gamma_i \\ \beta_i \\ \alpha_i \\ \sigma_i \end{pmatrix} = \begin{pmatrix} 0 \\ 0 \\ 125,000 ft \\ Mach\ 8 \\ -1.3^\circ \\ 0 \\ 0 \\ 0 \end{pmatrix} \tag{24}$$

The endpoint equation does not need to fully describe the state vector, only the conditions that are

necessary for a safe transition and landing. The manifold can be as simple as the following:

$$\mathbf{e}(\mathbf{x}(t_f), t_f) = \begin{bmatrix} z_f \\ V_f \end{bmatrix} = \begin{bmatrix} 500 \;\; ft \\ Mach \;\; 0.15 \end{bmatrix} \tag{25}$$

The vector above does not specify the final angles of attack or bank and it is possible that the vehicle could arrive at the ending manifold in an unrecoverable position (high angles of attack and bank along with large vertical speed). To prevent this from occurring, it is good practice to fully specify these variables as well as the associated acceptable range of values at the end point. Initial trajectories computed appear to be feasible trajectories but upon closer inspection met the end point manifold with vertical speeds exceeding $20,000\frac{ft}{min}$. The endpoint manifold was then modified to an endpoint set limited to vertical speeds between $-1500\frac{ft}{min} \leq \dot{z} \leq 500\frac{ft}{min}$ to represent a TAEM interface. Path constraints are derived primarily from the design and mission considerations of the vehicle and can be written as

$$\begin{bmatrix} -3g \\ -\infty \end{bmatrix} \leq \begin{bmatrix} \text{NormalForce(t)} \\ \text{TrimDeficiency(t)} \end{bmatrix} \leq \begin{bmatrix} 6g \\ 0 \end{bmatrix} \tag{26}$$

Equation 26 places a typical constraint on normal force and additionally constrains the vehicle's path to reside in a location in Mach-α space where the vehicle can be rotationally trimmed. There are also limits placed on the state vector and controls:

$$\begin{bmatrix} -\infty ft \\ -\infty ft \\ 0 ft \\ 0\frac{ft}{sec} \\ -\frac{\pi}{2} rad \\ -\infty rad \\ -10^\circ \\ -\frac{\pi}{2} rad \end{bmatrix} \leq \mathbf{x} \leq \begin{bmatrix} \infty ft \\ \infty ft \\ \infty ft \\ \infty\frac{ft}{sec} \\ \frac{\pi}{2} rad \\ \infty rad \\ 50^\circ \\ \frac{\pi}{2} rad \end{bmatrix} \tag{27}$$

$$\begin{bmatrix} -40\frac{\text{deg}}{sec} \\ -40\frac{\text{deg}}{sec} \end{bmatrix} \leq \mathbf{u} \leq \begin{bmatrix} 40\frac{\text{deg}}{sec} \\ 40\frac{\text{deg}}{sec} \end{bmatrix} \tag{28}$$

The limits that have values of plus and minus infinity represent states without hard limits and the constraint on the altitude component of the state vector is imposed to prevent premature contact with the ground.

VII. Results

The following sections discuss the footprint and individual trajectory analysis for several cost functions. Unless otherwise specified, the trajectories for both failed and nominal vehicles use the same initial conditions of

$$\mathbf{e}(\mathbf{x}_i, t_i) = [x_i \;\; y_i \;\; z_i \;\; V_i \;\; \gamma_i \;\; \beta_i \;\; \alpha_i \;\; \Phi_i]^T = [0\; ft \;\; 0\; ft \;\; 125\; kft \;\; Mach\; 8 \;\; -1.3^\circ \;\; 0^\circ \;\; 0^\circ \;\; 0^\circ]^T \tag{29}$$

These initial conditions correspond to a point on the entry trajectory after the peak heating and dynamic pressure and are suitable for failure analysis as the vehicle can begin to use its control surfaces to control the trajectory. The endpoint conditions for both trajectories are of the form

$$\begin{aligned} \mathbf{e}(\mathbf{x}_f, t_f) &= [x_f \;\; y_f \;\; z_f \;\; \dot{z}_f \;\; V_f \;\; \beta_f \;\; \Phi_f]^T \\ &= \left[free \;\; free \;\; free \;\; -500 \pm 1000\frac{ft}{min} \;\; Mach\; 0.15 \pm 0.003 \;\; free \;\; 0 \pm 20^\circ\right]^T \end{aligned} \tag{30}$$

Both vehicles observe a normal force constraint of -3 to 6 g's. The vehicle experiencing a control surface failure must observe the trim deficiency path constraint while the nominal vehicle is unconstrained by trim deficiency because as shown in Figure 1, the vehicle has adequate control power to trim over the entire flight envelope.

For the maximum downrange cases, the following trajectories for the nominal and failed vehicle were conducted as part of the rough footprint analysis. The performance criterion for these trajectories was to maximize the downrange position at the end of the trajectory. The Mach-altitude profiles for both trajectories are shown in Figure 6. Notice that the nominal trajectory trades excess speed for altitude. At the top of the zoom climb, the vehicle assumes the best lift/drag configuration and continues to the surface. The trajectory for the vehicle with the locked flap is prevented from using the same combination of angle of attacks as the nominal vehicle because of the imposed trim deficiency requirement. The trajectory does use the largest allowable angle of attack but this is insufficient to produce the zoom climb observed in the nominal trajectory. The novel section of this work is the inclusion of state-dependent constraints into the optimization problem, in particular, the trim deficiency maps. Recall, that it is desired that the reshaped trajectory lie in a region in the Mach-α space where the vehicle is rotationally trimmable, if physically possible. The restricted region in Mach-α space, due to the moment trim deficiency for the vehicle with stuck flaps, imposes severe trajectory performance penalties as shown in Figures 2 and 3. Figure 7 shows the differences between the two trajectories in Mach-α space as well as providing visual verification that the trajectory for the vehicle experiencing flap failure does not violate the imposed trim deficiency constraint of 0.003 and instead closely follows the contour in regions where the constraint is active. As can be seen in Figure 7, the nominal trajectory (blue) resides well within the non-trimmable region, while the reshaped trajectory (red) resides on the boundary between the trimmable and non-trimmable regions. Hence, state-dependent constraints have been successfully incorporated into the optimization problem. Similarly, Figure 8 shows the trajectories for the nominal and failed vehicle in Mach-α space when maximum crossrange is selected as the cost function. Again, the nominal (blue) trajectory violates the trimmability constraint, while the reshaped trajectory (red) is entirely within the trimmable region.

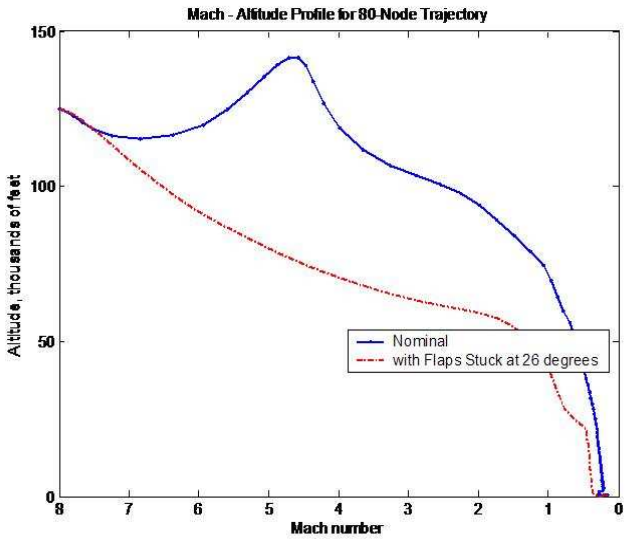

Figure 6. Maximum Downrange Mach-Altitude Profile.

VIII. Conclusions

This work consisted of the computation of new feasible trajectories for an air vehicle when a failure, such as a stuck control effector, has occurred. Once the failure has been identified, its effects on the trimmablility of the vehicle are determined and a trim deficiency map is constructed. In the cases investigated here, this map is a function of Mach number and angle of attack. Mach number is a state (actually, it is a scaled version of a state), so, to incorporate the trim deficiency into the optimization problem, state dependent constraints must be used. Results show that the incorporation of state dependent constraints is possible and the recomputed trajectory will avoid, if physically possible, regions where the vehicle is not rotationally trimmable.

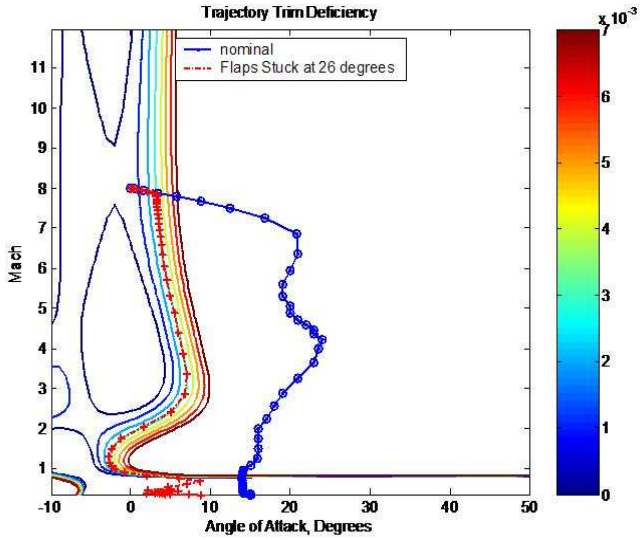

Figure 7. Trim Deficiency Map With Max Downrange Trajectories.

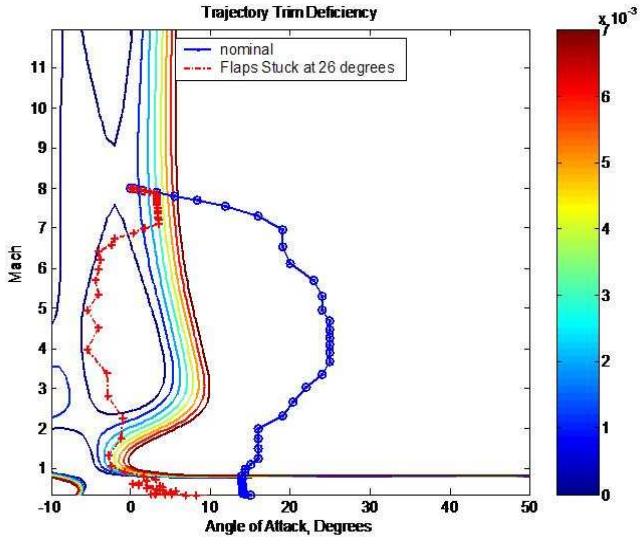

Figure 8. Trim Deficiency Map With Max Crossrange Trajectories.

References

[1]Schierman, J. D., Ward, D. G., Hull, J. R., Gandhi, N., Oppenheimer, M. W., and Doman, D. B., "Integrated Adaptive Guidance and Control for Re-Entry Vehicles with Flight-Test Results," *Journal of Guidance, Control and Dynamics*, Vol. 27, No. 6, 2004, pp. 975–988.

[2]Wiesel, W. E., *Spaceflight Dynamics*, McGraw-Hill, New York, NY, 1989.

[3]Pontryagin, L., *The Mathematical Theory of Optimal Processes*, Interscience Publishers, New York, NY, 1961.

[4]Bolender, M. and Doman, D. B., " Non-linear Control Allocation Using Piecewise Linear Functions," *Proceedings of the 2003 Guidance, Navigation and Control Conference*, AIAA Paper No. 2003-5357, August 2003.

[5]Oppenheimer, M., Doman, D., and Bolender, M., "A Method for Estimating Control Failure Effects for Aerodynamic Vehicle Trajectory Retargeting," *Proceedings of the 2004 AIAA Guidance, Navigation and Control Conference*, AIAA Paper No. 2004-5169, August 2004.

[6]Joselyn, S. B., *Optimization of Low Thrust trajectories with Terminal Aerocapture*, Master's thesis, Naval Postgraduate School, 2003.

[7]Canuto, C., Hussaini, M. Y., Quarteroni, A., and Zang, T. A., *Spectral Methods in Fluid Dynamics*, Springer Verlag, New York, New York, 1988.

[8]Ross, I. M. and Fahroo, F., "A Direct Method for Solving Nonsmooth Optimal Control Problems," *Proceedings of the 2002 World Congress of The International Federation on Automatic Control*, July 2002.

[9]Gottlieb, D., Hussaini, M. Y., and Orszag, S. A., "Theory and Applications of Spectral Methods," *Spectral Methods for PDE's*, SIAM, 1984.

[10]Elnagar, J., Kazemi, M. A., and Razzaghi, M., "The Pseudospectral Legendre Method for Discretizing Optimal Control Problems," *IEEE Transactions on Automatic Control*, Vol. 40, No. 10, 1995, pp. 1793–1796.

[11]Fahroo, F. and Ross, I. M., "Second Look at Approximating Differential Inclusions," *Journal of Guidance, Control and Dynamics*, Vol. 24, No. 1, 2001, pp. 131–133.

[12]Fahroo, F. and Ross, I. M., "Costate estimation by a Legendre Pseudospectral Method," *Journal of Guidance, Control and Dynamics*, Vol. 24, No. 2, 2001, pp. 270–277.